DJS Vol. 50(1)(2025) –pp.147-164 ISSN: 1012-5965

Delta Journal of Science
Available online at
https://djs.journals.ekb.eg/

Research Article

Zoology

The role of Myo-inositol in improving insulin resistance disorder induced in a high fat diet mouse model

Haneen M. Algazerey*; Mona M. Elwan; Hala A. Mostafa; Zainab A. Attia; Ghada A. Tabl

Department of Zoology-Faculty of science- Tanta University- Tanta –Egypt

***Corresponding author:** Haneen M. Algazerey **e-mail:** haneenmahmoud68199@gmail.com
Received: 20/5/2025 **Accepted:** 14/6/2025

KEYWORDS

C57/BL6; obesity; High fat diet; insulin resistance; myo-inositol.

ABSTRACT

Recently, the prevalence of insulin resistance (IR) has increased because of lifestyle (availability of fast food, office jobs, and internet). Myo-inositol (MI) was chosen to improve IR as it is present in a variety of foods, essential in several important processes of cell physiology, and synthesized de novo in humans during glycolysis from glucose-6-phosphate (G6P). The effects of MI on certain parameters in a diet-induced obesity mouse model were studied. The study was conducted on 49 male C57BL/6 mice weighing between (23±25 g) of 8 weeks of age and divided into 7 groups (7 mice per each). Group (GP) 1 kept as control with a normal diet and without any treatment, GP 2 received orally 1.2 mg/g of MI, GP 3 received orally 250 mg/kg of Metformin(Met), metformin was used as a reference drug, GP 4 received high-fat diet (HFD) without treatment, GP 5 received HFD with 1.2 mg/g of MI, GP 6 received HFD with 250 mg/kg of Met, GP 7 received HFD with 1.2 mg/g of MI with 250 mg/kg of Met. After 14 weeks of oral administration of MI in a high-fat diet (HFD)--fed C57BL/6 mice. The results showed significant reductions in total body weight, with no effect on lean body weight. Additionally, there was a decrease in serum alanine aminotransferase (ALT) and aspartate aminotransferase (AST) levels, as well as a decrease in urea and creatinine levels, and an improvement in insulin resistance in obese mice. Meanwhile, reductions in fasting blood glucose, and insulin levels were observed in myo-inositol-treated mice. These results suggest that myo-inositol may be a candidate for the treatment of insulin resistance.

Introduction

Insulin resistance (IR) is defined as an impaired body reaction to insulin-stimulated target cells, mostly found in the muscles, liver, and different kinds of adipose tissue **(Courtney *et al*., 2021)**. Insulin resistance reduces the body's ability to release glucose, which causes βcell insulin production to rise in response **(Schütten *et al*., 2020)**. Impaired insulin action, which reduces hepatic glucose production and increases glucose uptake in muscle and adipose tissue, is the hallmark of obesity-induced IR. It has been discovered that there is a causal relationship between obesity and insulin resistance, and that weight loss or gain may enhance or decrease insulin sensitivity **(Amin et al., 2019)**. The most common habit at the present time is a sedentary lifestyle, it is a key factor in the development of obesity. Modern lifestyles often involve extended periods of sitting, whether at work, during commuting, or during leisure activities (e.g., watching TV, using electronic devices **(Bashatah, et al., 2023).**

Hyperinsulinemia eventually spreads throughout the body as a result. Innate and chronic inflammatory reactions decreased endothelium layer function, hyperglycemia hypertension, dyslipidemia, visceral obesity, and disturbance of the hemostasis balance are among the effects of IR on metabolism **(Bartosiewicz *et al*., 2017).** Sometimes MI, referred to as inositol (cyclohexanehexol), is a six-hydroxyl grouped cyclic carbohydrate **(Razavi, 2024).** It was long thought to be vitamin B8, but because it is made of glucose, it is not regarded as a necessary food. The usual daily food intake of MI is between 0.5 and 1.0 g, with each kidney producing about 2 g of it **(Bevilacqua *et al*., 2018)**. In addition to kidneys, the liver and brain also manufacture MI, but in far smaller quantities. Crucially though, MI concentrations in the brain can reach 10- to 15-fold higher than in the blood, and there is little uptake of MI from the systemic circulation **(Bevilacqua et al., 2018).** Myo-inositol is often studied for its potential benefits in conditions such as polycystic ovary syndrome (PCOS), metabolic disorders, and mental health issues like anxiety and depression. It is also commonly used as a dietary supplement, sometimes in combination with other compounds like folic acid **(Ahanger et al., 2024)**.

This study is aimed at assessing the impact of myo-inositol administration on high-fat diet-induced insulin resistance in C57/BL/6 mice.

Materials and methods

Sample collection

All animal experimentation was approved by the animal committee and met all guidelines for its use (Institutional Animal Care and Use Committee (IACUC)) and was conducted in accordance with ethical standards approved at the Zoology department, Faculty of Science, Tanta University (IACUC-SCI-TU-0334). Male C57BL/6 mice, 8-week-old and weighing 23±2g, were raised in a standard environment. After one week of acclimation feeding, only those in good health were randomly assigned to seven groups: the 3 standard chow diet group (Ctrl group, Crtl group+ MI, Crtl group+ Metformin (Met)) and the high-fat diet (HFD) group was made up of 5:2:0.07: 0.07 ratios of commercial mice chow, sugar, lipids from lamps, and white

bread. After 3 weeks of HFD feeding, fasting insulin and HOMA-IR were measured. Six weeks later, the mice in Ctrl group and high-fat diet group were treated with MI at a dose of 1.2mg/g) **(Zhang, et al., 2019)** and 250 mg/kg from Met **(Cefalu et al., 2013)** orally.

Growth parameters measurement

The markers used to assess the development of obesity include body weight and waist circumference. The body weight and waist circumference were recorded every week.

Biochemical analysis

At the end of the experiment, every week mice were weighed, and their waists were measured. Following the course of treatment, mice that had fasted overnight were weighed, sacrificed by cervical dislocation, and blood samples were taken. Blood samples were centrifuged using a Hettich Zentrifugen Tuttlingen centrifuge for ten minutes at 4000 r.p.m. Serum was separated into portions in order to measure the following: fasting insulin (was evaluated according to **Miller et al., (2009)** additionally, fasting blood glucose (was assessed according to **Burtis, (2006**). Moreover, HOMA_IR.Alanine aminotransferase (ALT), aspartate aminotransferase (AST), and serum creatinine which were determined according to **Burtis, (2006**). Finally, the serum urea was determined according to **Adeyemi et al., (2015**).

Histopathological investigations

Immediately after dissection, liver and kidney were removed, washed in saline, and put in formalin solution (10% neutral buffered) for 2 days, paraffin embedded, and sectioned. The sections were then stained with hematoxylin and eosin, and the results were seen under a light microscope **(Utete et al., 2019).**

Statistical analysis

Data were expressed as mean± standard deviation of the mean (n=5). Differences between groups were determined using one-way ANOVA followed by Tukey test and post hoc test. Significant differences were indicated by p- values <0.05.

Results

Growth Parameters

The group IR showed the highest weight and waist, significantly higher than all other groups. The control/metformin group had the lowest weight and waist, which was significantly lower than the control and control/myo-inositol groups. IR/myo-inositol/metformin had lower weight and waist compared to IR but was not significantly different from IR/myo-inositol and IR/metformin.

Glucose homeostasis parameters

The group of IR had the highest fasting blood glucose (FBG) and fasting insulin level, significantly higher than all other groups. The IR/myo-inositol/metformin group had the lowest fasting blood glucose and fasting insulin, significantly lower than the IR group and comparable to other treatment groups. The control and control/metformin groups had similar fasting glucose levels and fasting insulin, both significantly different from the IR group but not from each other.

The group of IR had the highest HOMA-IR value, indicating the highest level of insulin resistance.IR/myo-inositol, IR/metformin, and IR/myo-inositol/ metformin groups had significantly lower HOMA-IR values, suggesting reduced insulin resistance. The IR/myo-inositol/metformin group had the highest HOMA-IR among these treatment groups but is still significantly lower than the IR group. Control and control/myo-inositol have similar

HOMA-IR values, which were but not from each other.
significantly different from the IR group

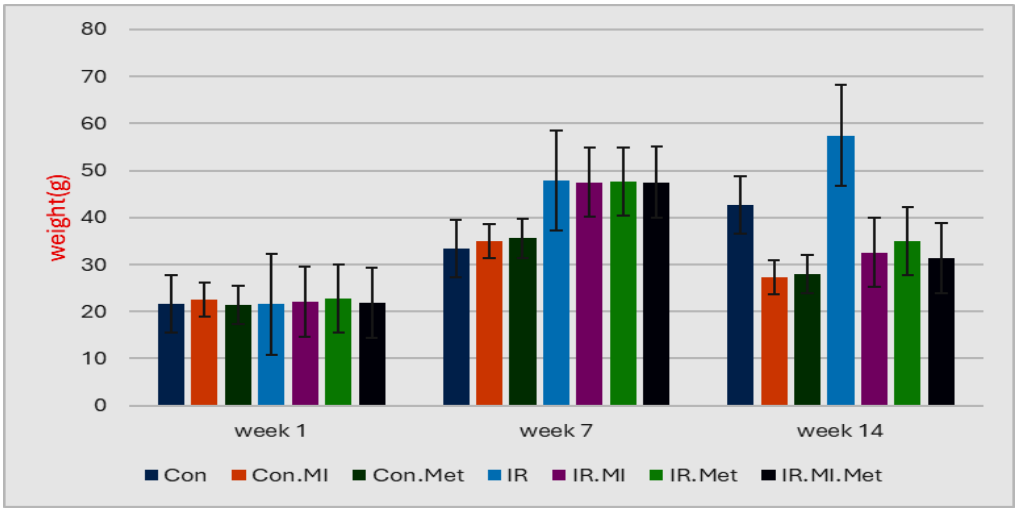

Fig. (1): Growth parameter (weight) in week 1,7,14 in control groups, untreated and treated groups with MI, Met and MI+Met. Data showed as mean ±SD**.**

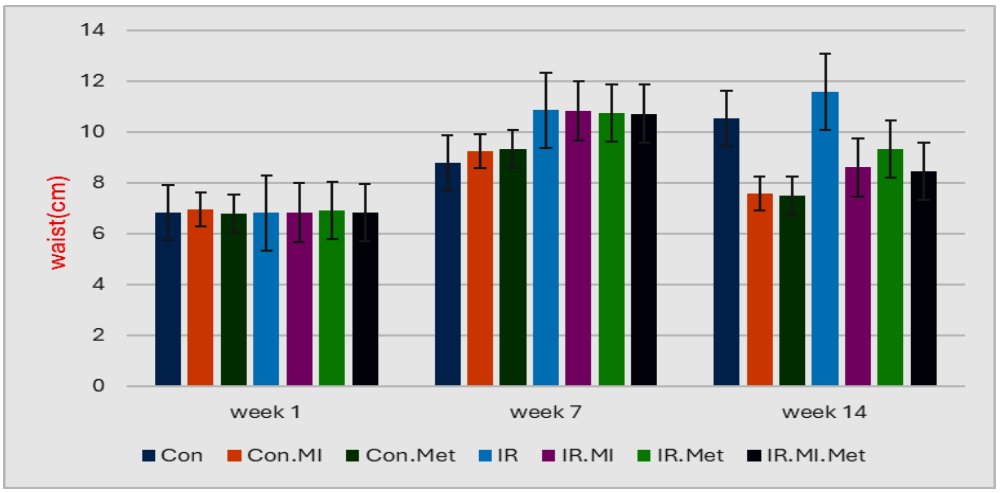

Fig. (2): Growth parameter (waist) week 1,7.14 in control groups, untreated and treated groups with MI, Met and MI+Met. Data showed as mean ±SD.

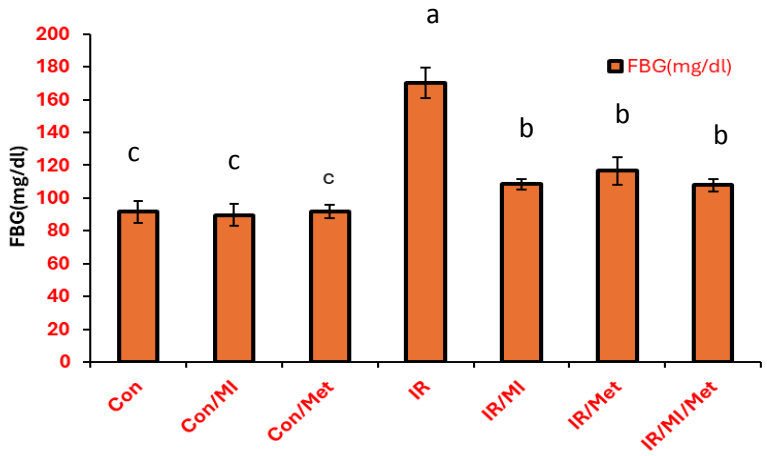

Fig. (3): Fasting blood glucose in control groups, untreated and treated groups with MI, Met, and MI+Met. Data showed as mean ±SD. Different letters indicate significant differences among the columns ($p>0.05$); a: significant with untreated group, b: significant with treated groups IR +MI, IR+Met, IR+MI+Met, c: significant with control, control +MI and control +Met groups.

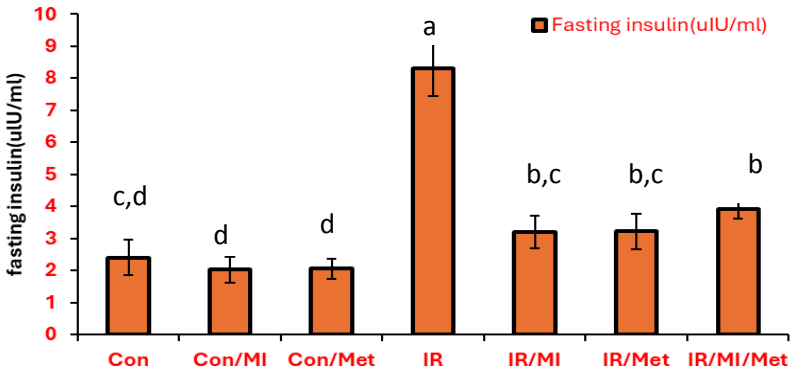

Fig. (4): Fasting insulin in control groups, untreated and treated groups with MI, Met, and MI+Met. Data showed as mean ±SD. Different letters indicate significant differences among the columns ($p>0.05$) a: significant with untreated group, b: significant with treated groups IR +MI, IR+Met, IR+MI+Met, c: significant with control group, d: significant with control +MI and control +Met groups.

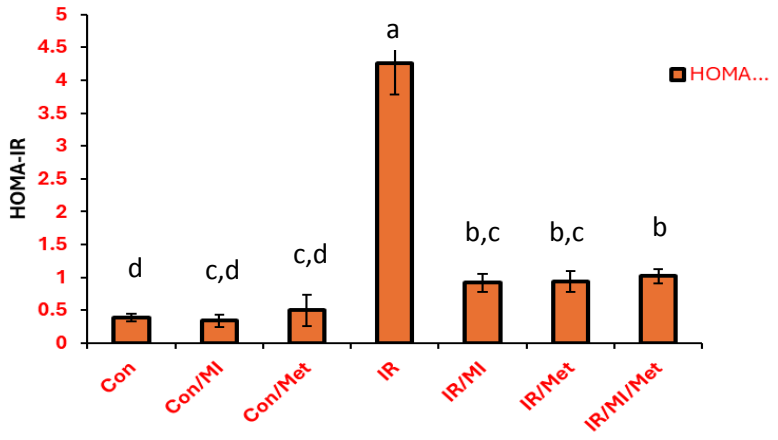

Fig. (5): HOMA-IR in control groups, untreated and treated groups with MI, Met, and MI+Met. Data showed as mean ±SD. Different letters indicate significant differences among the columns ($p>0.05$); a: significant with untreated group, b: significant with treated groups IR +MI, IR+Met, IR+MI+Met, d: significant with control group, control +MI and control +Met groups.

Liver and kidney function tests

The group of IR had the highest ALT, AST, serum creatinine, and serum urea activity, significantly higher than all other groups. IR/myo-inositol, IR/metformin, and IR/myo-inositol/metformin groups have lower ALT, AST, serum creatinine and serum urea activities, which were significantly lower than the IR group but similar to each other. Control, control/myo-inositol, and control/metformin groups had similar ALT, AST, serum creatinine, and serum urea levels, all significantly lower than the IR group but not significantly different from each other.

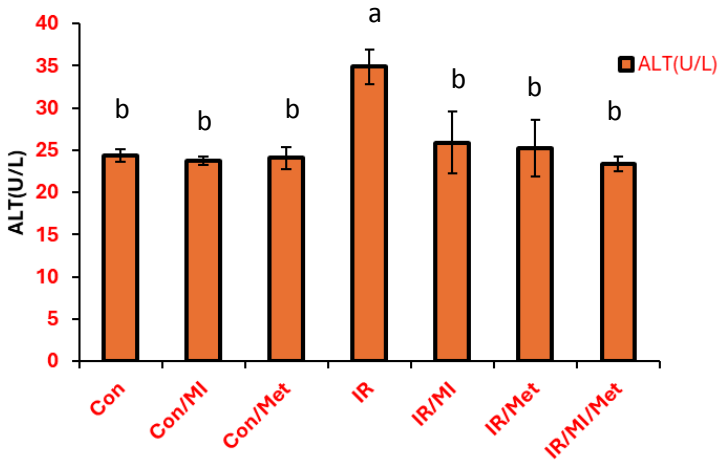

Fig. (6): ALT in control groups, untreated and treated groups with MI, Met, and MI+Met. Data showed as mean ±SD. Similar letters indicate non-significant differences among the columns ($p>0.05$); a: significant with untreated group, b: significant with control, control +MI, control +Met groups, treated groups IR +MI, IR+Met, and IR+MI+Met groups.

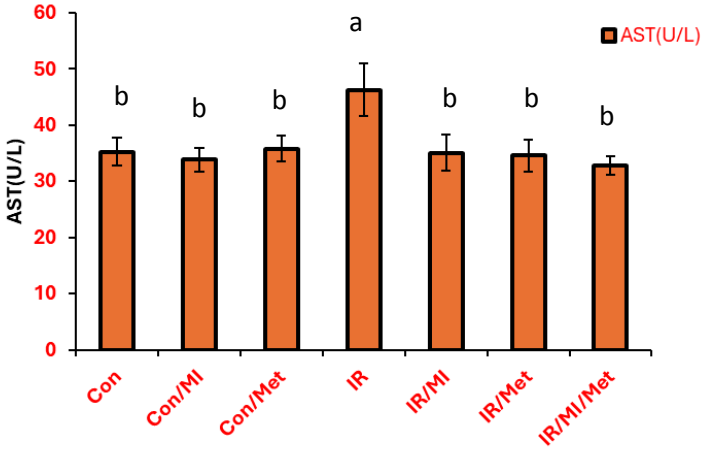

Fig. (7): AST in control groups, untreated and treated groups with MI, Met and MI+Met. Data showed as mean ±SD. Similar letters indicate non-significant differences among the columns ($p>0.05$); a: significant with untreated group, b: significant with control, control +MI, control +Met groups, treated groups IR +MI, IR+Met, and IR+MI+Met groups.

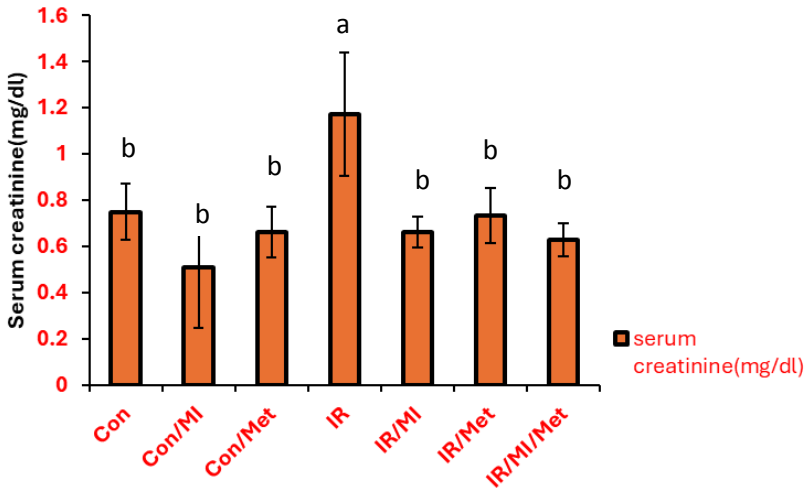

Fig. (8): Serum creatinine in control groups, untreated and treated groups with MI, Met, and MI+Met. Data showed as mean ±SD. Similar letters indicate non-significant differences among the columns ($p>0.05$); a: significant with untreated group, b: significant with control, control +MI, control +Met groups, treated groups IR +MI, IR+Met, and IR+MI+Met groups

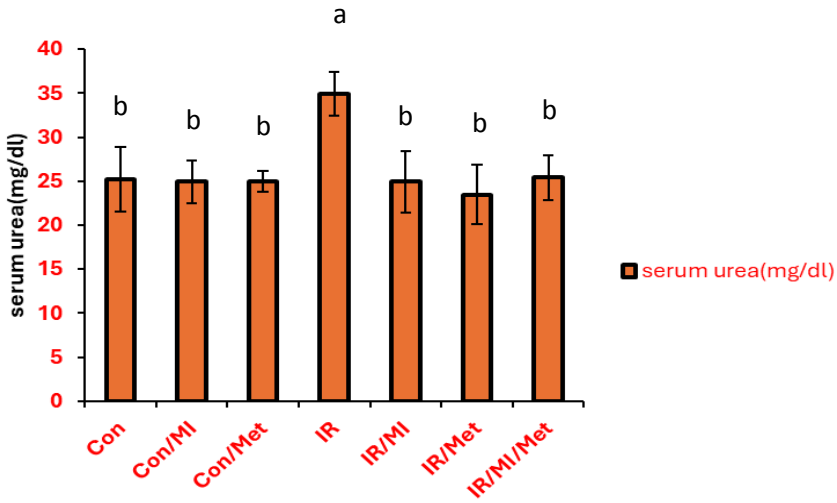

Fig. (9): Serum urea in control groups, untreated and treated groups with MI, Met and MI+Met. Data showed as mean ±SD. Similar letters indicate non-significant differences among the columns ($p>0.05$); a: significant with untreated group, b: significant with control, control +MI, control +Met groups, treated groups IR +MI, IR+Met and IR+MI+Met groups.

Histological examination

Liver

Light microscopic examination of liver sections of control mice showed normal hepatic parenchyma consisting of normal hepatocytes arranged in cords or strands around the central vein and separated with blood sinusoid which is lined with endothelial cells and Kupffer cells **(A)**. Liver sections of control mice treated with MI (G2) showed normal hepatocytes arranged in cords around the central vein, few numbers of hepatocytes with dark stained nuclei (pyknotic) and blood sinusoids were regular with normal Kupffer cells **(B).** Liver sections of control mice treated with Met (G3) showing normal like structure of the hepatic architecture; hepatocytes arranged in cords around the central vein, regular blood sinusoids with normal Kupffer cells **(C)**. Liver sections of diseased animals with IR(G4) show marked disorganization of the hepatic

structure; obvious degree of diffuse hepatic vacuolar changes consistent associated with focal mononuclear cell infiltration consisting mostly of lymphocytes and macrophages and blood sinusoids were deteriorated **(D)**. Liver sections of diseased mice treated with MI (G5) showed mild improvement of the hepatic structure; few numbers of hepatocytes were vacuolated and normal portal area was noticed **(E)**. Liver sections of diseased mice treated with Met (G6) showed noticed improvement of the hepatic structure; mild congested central vein, regular hepatic strands, decrease of the hepatic vacuolar changes within the cytoplasm of the hepatocytes and tiny foci of mononuclear cells aggregation **(F)**. Liver sections of diseased animals treated with MI +Met (G7) showing improvement of the hepatic construction; mostly hepatocytes (H) are normal with central localized nuclei, few numbers with granular eosinophilic changes and degenerated, also blood sinusoids were regular with normal Kupffer cells **(G).**

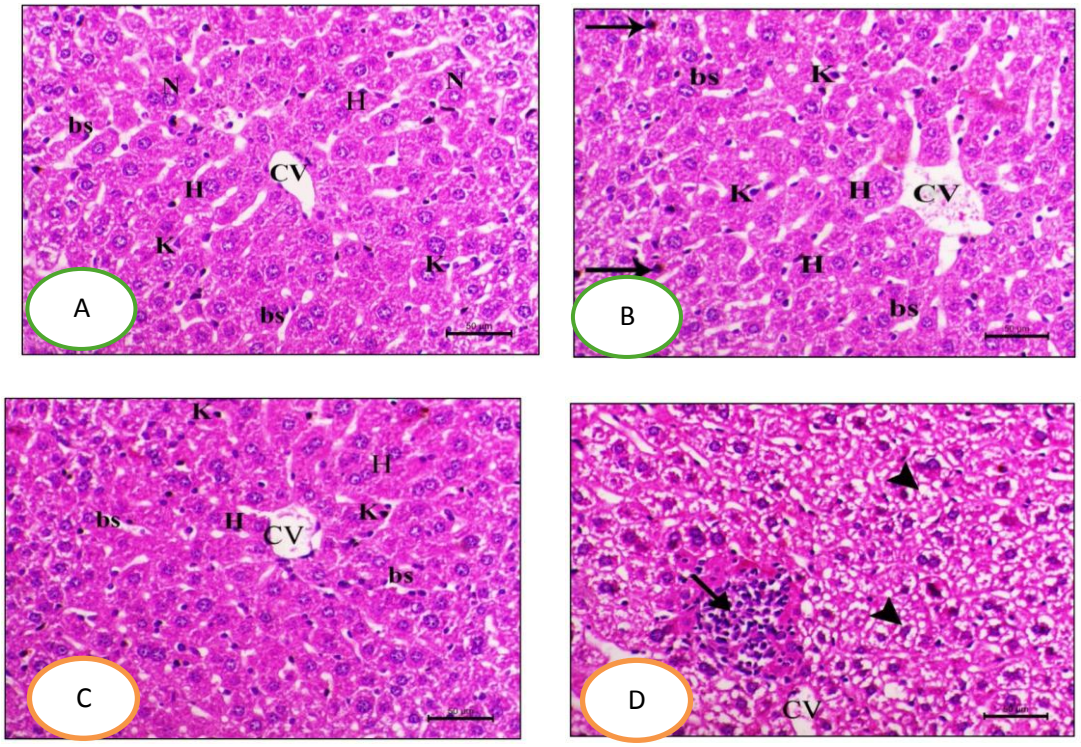

Figs (10, 11) (A- G**): Photomicrographs of liver sections of different experimental animal groups stained with (H&E), X 400, bar= 50 µm**

Fig. (10) A: Liver sections of control mice (G1) showing normal hepatic parenchyma; normal radiating cords of hepatocytes (H) with central nuclei (N), normal central vein (CV) and regular blood sinusoids (bs) lined with endothelial cells and Kupffer cells (K). **B**: Liver sections of normal mice treated with MI (G2) showing normal hepatocytes (H) arranged in cords around the central vein (CV), few numbers of hepatocytes with pyknotic nuclei (arrows) and regular blood sinusoids (bs) with normal Kupffer cells (K). **C**: Liver section of normal animal treated with Met (G3) showing normal like structure of the hepatic architecture; regular central vein (CV), normal radiating hepatocytes (H), regular blood sinusoids (bs) lined with normal Kupffer cells (K). **D**: Liver sections of diseased animal with IR (G4) showing marked disorganization of the hepatic structure; irregular central vein (Cv), mostly hepatocytes with vacuolated or degenerated cytoplasm (arrowhead), severe aggregation of monocellular infiltration (arrow) and blood sinusoids are deteriorated.

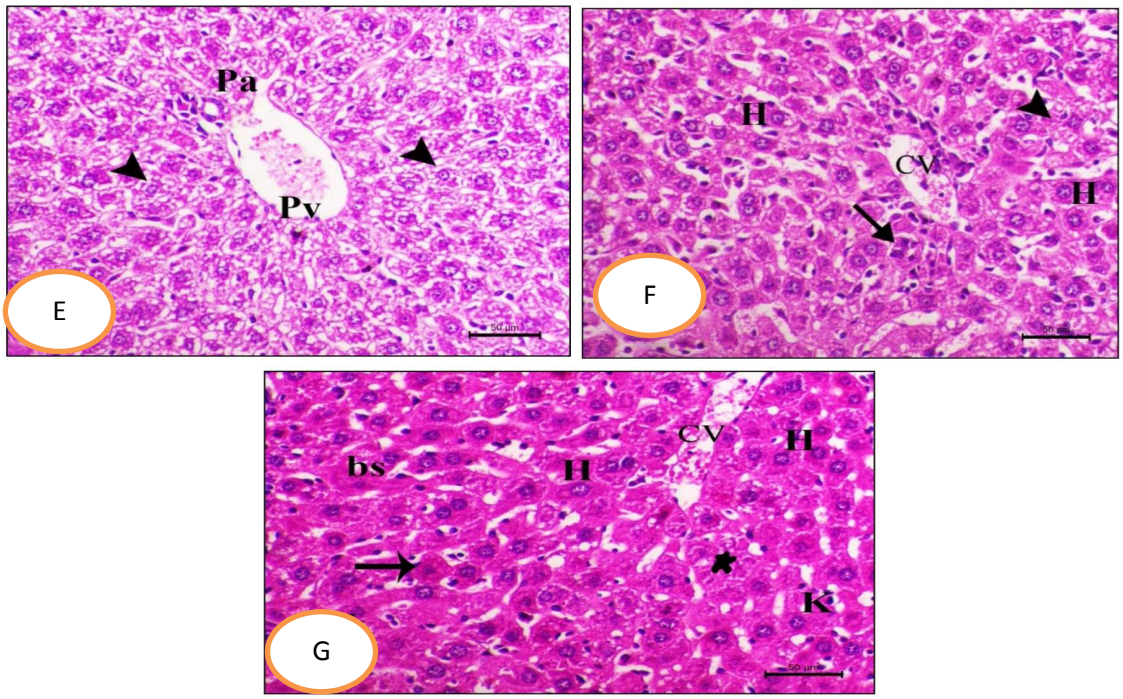

Fig. (11). E: Liver sections of diseased mice treated with MI (G5) showing few numbers of hepatocytes with cytoplasmic vacuolation (arrowheads), normal portal area with regular portal vein (Pv) (X 400). **F:** Liver sections of diseased mice treated with Met (G6) showing noticed improvement of the hepatic structure; mild congested central vein (Cv), regular hepatic strands (H), decrease of the hepatic vacuolar changes within the cytoplasm of the hepatocytes (arrowhead) and tiny foci of mononuclear cells aggregation (arrow) (X 400). **G:** Liver sections of diseased mice treated with MI+Met (G7) showing improvement of the hepatic construction; dilated and mild congested central vein (CV), mostly hepatocytes (H) are normal with central localized nuclei, few numbers with granular eosinophilic changes (arrows) and degenerated (star), also blood sinusoids are regular with normal Kupffer cells (K) (X 400).

Kidney

Histology of Kidney sections of control animal (G1) showing normal renal glomeruli (G) and tubules (PT indicates normal proximal renal tubules and DT indicates normal distal renal tubules), **(H).** Kidney section of normal animal treated with MI (G2) showing normal renal glomeruli (G) and tubules (PT indicates proximal renal tubules and DT indicates distal renal tubules), **(I).** Kidney section of normal animal treated with Met (G3) showing normal renal glomeruli (G) and tubules (PT indicates proximal renal tubules and DT indicates distal renal tubules), **(J).** Kidney section of diseased animal with IR (G4) showing marked tubular degeneration associated with fatty vacuolation of the renal tubular epithelium (arrowhead) and interstitial mononuclear inflammatory cell infiltration consisting of lymphocytes and macrophages (arrow) (G indicates renal glomeruli), **(K).** The kidney section of diseased animals treated with MI (G5) showed a decrease the degenerative fatty changes (arrowheads) and inflammatory cell infiltration (G indicates renal glomeruli), **(L).** Kidney section of diseased animals treated with Met (G6) showing limited periglomerular vacuolar changes within the renal tubular epithelium (arrowhead) (G indicates renal glomeruli), **(M).** Kidney section of an HFD animal treated with MI+Met (G7) showed a marked

decrease in the degenerative and inflammatory lesions within the renal tissues, with mild vacuolar degenerative changes (arrowheads) (G indicates renal glomeruli), **(N).**

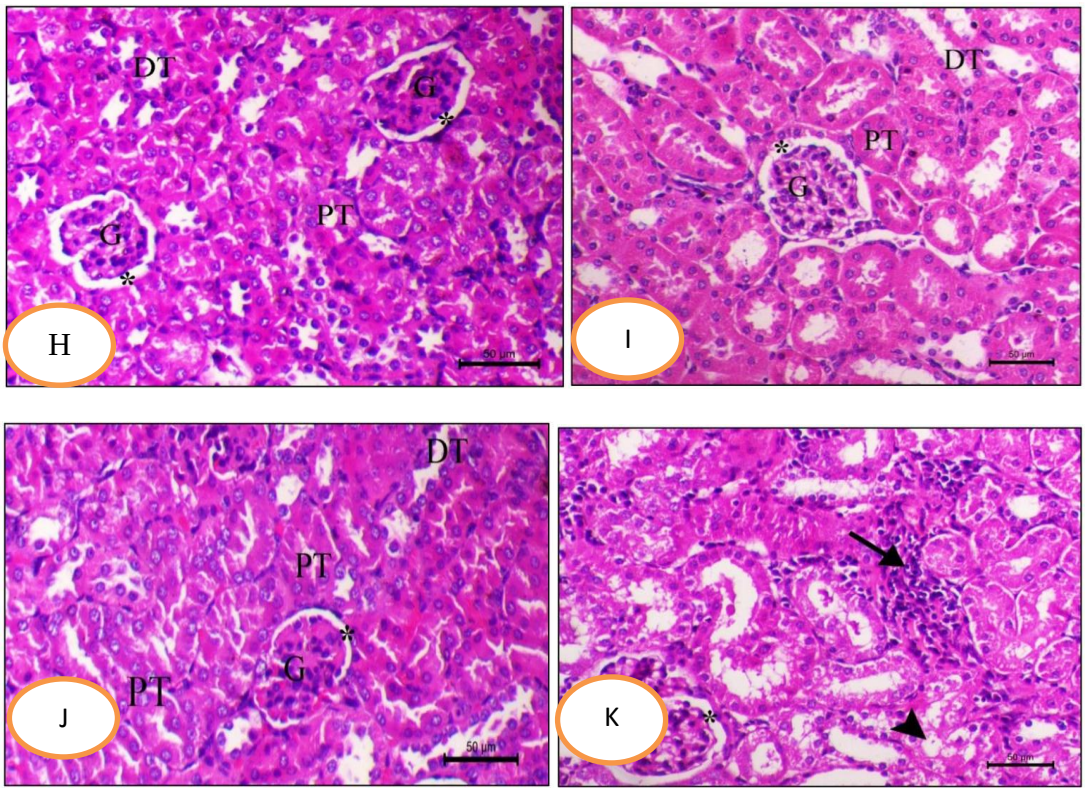

Figs. (12, 13)(H-M): Photomicrographs of kidney sections of different experimental animal groups stained with H& Estain, (X400).

Fig. (12). H: Kidney section of control animal (G1) showing normal renal glomeruli (G) with regular Bowman's space (*) and renal tubules (PT indicates normal proximal renal tubules and DT indicates normal distal renal tubules), X400, bar= 50 µm**. I:** Kidney section of normal animal treated with MI (G2) showing normal renal glomeruli (G) with regular Bowman's space (*) and normal tubules (PT indicates proximal renal tubules and DT indicates distal renal tubules), X400, bar= 50 µm. **J:** Kidney section of normal animal treated with Met (G3) showing normal renal glomeruli (G) with regular Bowman's space (*), mostly proximal renal tubules are normal (PT), but few numbers of distal convoluted tubules are distended (DT), X 400, bar= 50 µm. **K:** Kidney section of diseased animal with IR(G4) showing marked disorganization of the renal tissue; disorganized glomeruli (G) with irregular Bowman's space (*), noticeable tubular degeneration associated with fatty vacuolation of the renal tubular epithelium (arrowhead) and interstitial mononuclear inflammatory cells infiltration consisted of lymphocytes and macrophages (arrow), X400, bar= 50 µm.

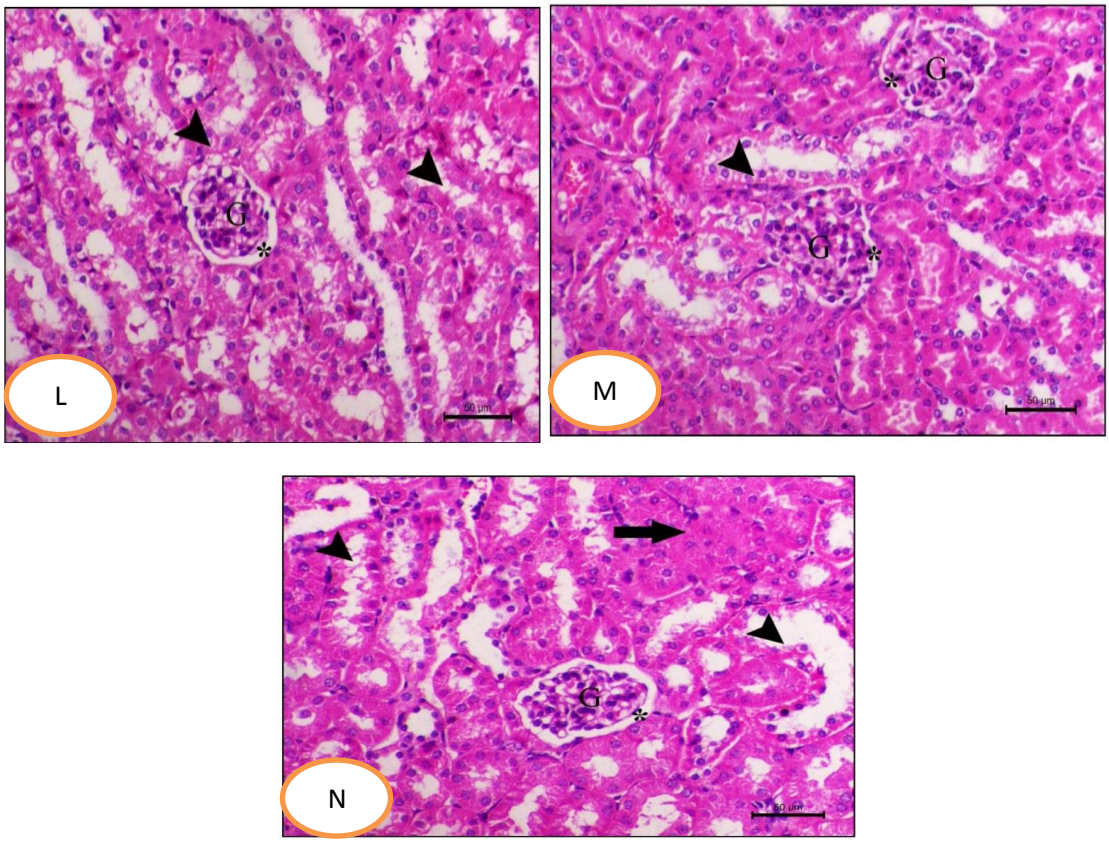

Fig. (13)L: Kidney section of diseased animal treated with MI (G5) showing improvement of the renal tissue; normal glomeruli (G) with regular Bowman's space (*), few numbers of renal tubules with degenerative lining epithelia (arrowheads) and decrease of the inflammatory cell's infiltration, X 400, bar= 50 µm. **M:** Kidney section of diseased animal treated with Met (G6) showing mild improvement of the renal structure; abnormal glomeruli (G) with irregular Bowman's space (*), limited periglomerular vacuolar changes within the renal tubular epithelium (arrowhead), X 400, bar= 50 µm. **N:** Kidney section of HFD animal treated with MI+ Met (G7) showing normal organized glomeruli (G) with regular Bowman's space (*) marked decrease the degenerative and inflammatory lesions within the renal tissues, few number of renal tubules with mild vacuolar degenerative changes (arrowheads), some tubules their contents are intermixed with each other's (thick arrow) X 400, bar= 50 µm.

Discussion

This present study was designated to investigate the therapeutic effects of myo-inositol (MI) on HFD-induced insulin resistance in C57BL/6 mice at different levels, growth parameters, glucose homeostasis, liver functions, kidney functions, and histological examinations. C57BL/6 mice that were given a high-fat diet were frequently utilized in studies on the causes, prevention, and treatment of obesity. There is a metabolic disease linked to the C57BL/6 phenotype.

Additionally, **Recena et al., (2019)** examined how a high-fat diet could induce non-alcoholic fatty acid liver disease (NAFLD) in mice of the C57BL/6 strain, the strain most frequently utilized for this experimental illness model. High-fat diet intake allows animals to develop obesity, hyperinsulinemia, hyperglycemia **(White et al., 2013)**, hypertension

(Recena et al., 2019), and liver damage, similar to the phenotype observed in humans with NAFLD. In this study, after 14 weeks of treatment, the body weight of C57BL/6 mice was significantly higher than that of ctrl mice. The weight of MI-treated mice was reduced significantly after 12 weeks, compared with IR mice. These results are consistent with **Aghajani et al., (2024)** as they assessed the influence of MI supplementation on IR through AMP-activated protein kinase/phosphoinositol-3-kinase/protein kinase-B (AMPK/PI3K/AKT) signaling pathway in obese patients with NAFLD. Insulin resistance is considered a cause, an outcome, or even an epiphenomenon of NAFLD. The AMPK/PI3K/AKT pathway influences β-cell function and controls the activity of molecular mediators involved in cellular homeostasis, especially in insulin-sensitive tissues, in the context of metabolic-endocrine illness.

Excess body weight, especially in abdominal obesity, plays a central role in the development of IR (**Dutta et al., 2024)**. Weight alone may not provide a full picture of metabolic health, as fat distribution is equally important. Abdominal fat, often measured by waist circumference, is a more significant risk factor for metabolic dysfunction than overall body weight.

The current study indicated that growth parameters significantly decreased in ctrl, IR + MI, and IR +Met groups compared to the IR group. These results are consistent with an earlier study MI has been reported to influence metabolic syndrome and abdominal fat, particularly visceral fat **(Raheem et al., 2022).** Also, **(Dinicola et al., 2024)** found women who suffer from Polycystic ovary syndrome (PCOS) are prone to visceral obesity. Myo-inositol supplementation had been associated with a reduction in waist circumference, reflecting a reduction in visceral fat.

Fasting blood glucose (FBG) is one of the primary indicators used to assess glucose homeostasis. In insulin resistance, the body's tissues (e.g., muscle, liver, and adipose tissue) become less responsive to insulin, which leads to elevated blood glucose levels. As insulin resistance progresses, the pancreas compensates by increasing insulin secretion, which leads to hyperinsulinemia. Despite this compensatory mechanism, fasting blood glucose tends to rise over time because insulin cannot effectively drive glucose into the cells **(Chaudhary et al., 2024).** In insulin resistance, both fasting blood glucose and fasting insulin levels are elevated, leading to an increased HOMA-IR score. A higher HOMA-IR indicates greater insulin resistance **(Carobene et al., 2025).**

In the present study, Insulin resistance mice showed a significant elevation in fasting blood glucose, fasting insulin, and HOMA-IR compared to control, IR with MI, and IR with Met groups, this agrees with a previous study by (**Yang et al., 2025)** who discussed that increase in fasting glucose level is due to the ability of insulin to inhibit hepatic glucose production (by glycogenolysis and gluconeogenesis).

To discuss the previous results, myo-inositol has been shown to improve glucose homeostasis in animal models of insulin resistance. By improving insulin signaling, it enhances the efficiency of glucose uptake in peripheral tissues like muscle and adipose tissue **(Hsu et al., 2022)**. It also reduces hepatic glucose

production, helping lower fasting blood glucose. Moreover, it has been shown to lower insulin levels and HOMA-IR, a sign of insulin resistance, which lowers the risks of metabolic syndrome **(Lepore et al., 2021)**. However, research by **Croze et al., (2013)** demonstrated that there was no positive impact from myo-inositol administration. Myo-Inositol appears to have affected adipose tissue by inhibiting de novo lipogenesis instead of inducing lipolysis. This could help to explain why myo-inositol is ineffective at reducing adipose tissue mass in situations when de novo lipogenesis is decreased (high-fat diet feeding) or obesity is already well-established (aged mice). The generation of inositol glycan putative insulin second messengers was probably reduced in context of insulin resistance which may explain the reduced effect of myo-inositol in both obese mice models. Moreover, myo-Inositol did not prevent lipotoxicity and so associated insulin resistance in high-fat diet -fed mice.

Also, the liver is sensitive to insulin. It develops insulin resistance before other organs do because it is a crucial regulator of glucose–glycogen balance, which is brought on by obesity **(Petersen et al., 2018)**. Since the liver is a crucial organ for maintaining glucose homeostasis throughout the body, studying the pathophysiology of insulin resistance in this organ may help manage diabetes and its related problems. The current study's findings showed that in comparison to the insulin resistance group, the control, IR with MI, and IR with Met groups had significantly lower serum ALT and AST levels. That is in agreement with **(Liu et al., 2025)** who demonstrated that propolis ethanol extract (PEE) ameliorated the reductions in body weight and liver index in aged mice. Propolis ethanol extract significantly reduced AST and ALT levels. The increase in AST and ALT of the IR mice indicated cells in muscles, fat and liver don't respond to insulin as they should**.** The two enzymes, AST and ALT which are secreted into the bloodstream by hepatocytes, indicate that hepatic damage has taken place **(Shakeri *et al.*, 2022)**, it can be caused by a variety of conditions, ranging from viral infections (hepatitis) to metabolic disorders (NAFLD) and drug-induced injury. While ALT is more liver-specific, AST can also provide valuable information, especially when considered alongside other clinical markers. Recent research continues to explore the underlying molecular pathways of liver injury, focusing on mechanisms such as immune responses, oxidative stress, and mitochondrial dysfunction **(Andrade et al., 2019).**

Additionally, the present study showed that creatinine and urea levels were significantly decreased in control, IR with MI, and IR with Met groups in comparison with the insulin resistance group, the results agreed with recent studies which have further elucidated the bidirectional relationship between insulin resistance and renal function. For instance, a longitudinal analysis by **(Otsuka et al., 2021)** demonstrated that individuals with insulin resistance exhibited a faster decline in estimated glomerular filtration rate (GFR) compared to insulin-sensitive counterparts. Additionally, a meta-analysis by **(Guo et al., 2024)** corroborated these findings, highlighting that insulin resistance significantly increases the risk of developing chronic

kidney disease (CKD). These studies underscore the importance of targeting insulin sensitivity as a potential therapeutic strategy for preserving renal health **(Otsuka et al., 2019; Guo et al., 2024).** In histological studies of the liver, these results showed reduced hepatic vacuolar changes, with improved hepatocyte appearance and less fat and glycogen infiltration in diseased animals treated with MI (G5) and both MI and Met help improve liver histology in insulin-resistant animals, with the combined treatment showing the most significant improvements compared to diseased animal with IR (G4): Liver shows hepatic vacuolar changes (fatty changes and glycogen infiltration) and inflammation with focal infiltration of mononuclear cells (mainly lymphocytes and macrophages). Furthermore, several studies have reported that Myo-inositol supplementation can help reduce hepatic fat accumulation **(Pani et al., 2021)**. Also, the results of **(Dinicola et al., 2021)** suggested that MI supplementation could decrease liver fat content and improve liver function markers in insulin-resistant individuals in PCOS women.

Histological examination of kidney tissue in insulin-resistant animals (G4) reveals significant damage, including tubular degeneration, fatty vacuolation, and inflammation, which are typical of kidney involvement in insulin resistance and associated conditions like diabetic nephropathy compared to treatment with Myo-inositol (G5) results in notable improvements by reducing fatty changes and inflammatory infiltrates. Metformin (G6) also improves kidney histology but to a lesser extent, showing limited vacuolar changes. However, when Myo-inositol and Metformin are used in combination (G7), the kidney tissue shows marked improvement, with reduced degeneration and inflammation, highlighting a potential synergistic effect between the two treatments. Moreover, (**D'Elia et al. 2022 & Artunc et al., 2016)** said that insulin receptor is expressed on renal tubular cells and podocytes and insulin signaling has important roles in podocyte viability and tubular function. Renal sodium transport is preserved in insulin resistance and contributes to the salt sensitivity of blood pressure in hyperinsulinemia.

Conclusion

This study proved that myo-inositol can be used as a safe and effective treatment for insulin resistance as there is an improvement in body weight, waist, and glucose homeostasis parameters. Also, MI with Met can be used as a supplement for liver dysfunction, kidney dysfunction, and lipid abnormalities.

Based on the above points, Myo-inositol offers a promising therapeutic option for managing insulin resistance, particularly in the context of metabolic disorders such as PCOS, NAFLD, and diabetic nephropathy. It helps to improve insulin sensitivity, reduce inflammation, and prevent organ damage, particularly in the liver and kidneys. The combination of Myo-inositol with other insulin-sensitizing drugs, such as Metformin, can further enhance its effectiveness. Given its safety profile, it can be recommended for use in both pre-diabetic and diabetic individuals.

References

Ahanger, I. A., Bashir, B., Wani, O. H., Hajam, I. B., & Dar, T. A. (2024). Diverse Biological Functions of Myo-inositol: A Neuro-Metabolite, Osmoprotectant, and Diagnostic Marker. In *Cellular Osmolytes: From Chaperoning Protein Folding to*

Clinical Perspectives. Singapore: SNS. (pp. 161-183).

Amin, M. N., Hussain, M. S., Sarwar, M. S., Moghal, M. M. R., Das, A., Hossain, M. Z., ... & Islam, M. S. (2019). How the association between obesity and inflammation may lead to insulin resistance and cancer. *Diabetes Metab Syndr: CRRJ*, *13*(2): 1213-1224.

Andrade, R. J., Aithal, G. P., Björnsson, E. S., Kaplowitz, N., Kullak-Ublick, G. A., Larrey, D., ... & European Association for the Study of the Liver. (2019). EASL clinical practice guidelines: drug-induced liver injury. *J. Hepatol.*, 70(6): 1222-1261.

Adeyemi, O. T., Osilesi, O., Adebawo, O. O., Onajobi, F. D., & Oyedemi, S. O. (2015). Variations in the levels of total protein, urea and ureate in weaned male albino rats fed on processed Atlantic horse mackerel. *Variations*, *5*(6): 29-39.

Aghajani, T., Arefhosseini, S., Ebrahimi-Mameghani, M., & Safaralizadeh, R. (2024). The effect of myo-inositol supplementation on AMPK/PI3K/AKT pathway and insulin resistance in patients with *NAFLD. Food Sci. Nutr*, *12*(10): 7177-7185.

Artunc, F., Schleicher, E., Weigert, C., Fritsche, A., Stefan, N., & Häring, H. U. (2016). The impact of insulin resistance on the kidney and vasculature. *Nat Rev. Nephrol*, *12*(12): 721-737.

Bashatah, A., Ali, W. S., & Al-Rawi, M. B. A. (2023). Attitudes towards exercise, leisure activities, and sedentary behavior among adults: a cross-sectional, community-based study in Saudi Arabia. *Medicina*, *59*(9): 1524.

Bartosiewicz, J., Kaminski, T., Pawlak, K., Karbowska, M., Tankiewicz-Kwedlo, A., & Pawlak, D. (2017). The activation of the kynurenine pathway in a rat model with renovascular hypertension. *EBM*, *242*(7):750-761.

Bevilacqua, A., & Bizzarri, M. (2018). Inositols in insulin signaling and glucose metabolism. *Int J. Endocrinol.*, 2018(1): 1968450.

Carobene, A., Kilpatrick, E., Bartlett, W. A., Calle, P. F., Coşkun, A., Díaz-Garzón, J., ... & Aarsand, A. K. (2025). The biological variation of insulin resistance markers: data from (EuBIVAS). *Clin. Chem. La.b Med. (CCLM)*, *63*(1):110-117.

Cefalu, W. T. (2001). Insulin resistance: cellular and clinical concepts. *EBM*, *226*(1): 13-26.

Chaudhary, A., Bansal, S., Saha, S., Arora, S., Akram, W., & Kumar, S. (2024). Phosphodiesterase Inhibitors for Diabetes: From Mechanistic Insights to Therapeutic Innovations. *NEM*, e02506882344901.

Croze, M. L., & Soulage, C. O. (2013). Potential role and therapeutic interests of myo-inositol in metabolic diseases. *Biochimie*, *95*(10): 1811-1827.

D'Elia, J. A., Bayliss, G. P., & Weinrauch, L. A. (2022). The diabetic cardiorenal nexus. *Int. J. Mol. Sci*., *23*(13): 7351.

Dinicola, S., Unfer, V., Facchinetti, F., Soulage, C. O., Greene, N. D., Bizzarri, M., ... & Wdowiak, A. (2021). Inositols: from established knowledge to novel approaches. Int. J. Mol Sci, *22*(19): 10575.

Dinicola, S., Unfer, V., Soulage, C. O., Yap-Garcia, M. I. M., Bevilacqua, A., Benvenga, S., ... & Facchinetti, F. (2024). D-chiro-inositol in clinical practice: A perspective from The Experts Group on Inositol in Basic and

Clinical Research (EGOI). *Gynecol. Obstet. Invest*., *89*(4): 284-294.

Ezz, A. M., Zaki, S., & Tabl, G. A. (2023). Anti-diabetic effects of pomegranate peel extract and L-carnitine on streptozotocin induced diabetes in rats. *BP J.*, *16*(3): 1827-1835.

Guo, J., Liu, C., Wang, Y., Shao, B., Fong, T. L., Lau, N. C., ... & Chen, H. (2024). Dose-response association of diabetic kidney disease with routine clinical parameters in patients with type 2 diabetes mellitus: a systematic review meta-analysis. *EClinicalMedicine*, *69*.

Hsu, M. H., Chen, Y. C., Sheen, J. M., & Huang, L. T. (2020). Maternal obesity programs offspring development and resveratrol potentially reprograms the effects of maternal obesity. *Int. J. Environ. Res. Public Health*, 17(5): 1610.

Lee, D., Kim, S. J., Choi, Y. J., Rho, Y. H., Kang, T. S., Kim, Y. G., & Kang, K. S. (2025). The Glucose-Lowering Effect of Mesembryanthemum crystallinum and D-Pinitol: Studies on Insulin Secretion in INS-1 Cells and the Reduction of Blood Glucose in Diabetic Rats. *Nutrients*, *17*(1): 193.

Lepore, E., Lauretta, R., Bianchini, M., Mormando, M., Di Lorenzo, C., & Unfer, V. (2021). Inositols depletion and resistance: Principal mechanisms and therapeutic strategies. *Int. J. Mol. Sci*,, *22*(13): 6796.

Liu, J., Tian, S., Wang, J., Sang, Q., Su, W., Wu, J., & Zai, F. (2025). Hepatoprotective effects of propolis ethanol extract on D-galactose-induced aging mice: A metabolomics and transcriptomics analysis focusing on insulin resistance pathways. *J. Funct. Foods*, *125*: 106668.

Miller, W. G., Thienpont, L. M., Van Uytfanghe, K., Clark, P. M., Lindstedt, P., Nilsson, G., ... & Insulin Standardization Work Group. (2009). Toward standardization of insulin immune assays. *Clin Chem*., 55(5):1011-1018.

Pani, A., Giossi, R., Menichelli, D., Fittipaldo, V. A., Agnelli, F., Inglese, E., ... & Scaglione, F. (2020). Inositol and non-alcoholic fatty liver disease: A systematic review on deficiencies and supplementation. *Nutrients*, *12*(11): 3379.

Raheem, J., Sliz, E., Shin, J., Holmes, M. V., Pike, G. B., Richer, L., ... & Pausova, Z. (2022). Visceral adiposity is associated with metabolic profiles predictive of type 2 diabetes and myocardial infarction. *Med. Commun.*, *2*(1): 81.

Razavi, S. A., Kalari, M., Haghzad, T., Haddadi, F., Nasiri, S., & Hedayati, M. (2024). Exploring the potential of myo-inositol in thyroid disease management: focus on thyroid cancer diagnosis and therapy. F*ront .Endocrinol*, *15*: 1418956.

Recena Aydos, L.. (2019). Nonalcoholic fatty liver disease induced by high-fat diet in C57bl/6 models. Nutrients, 11(12): 3067.

Saltiel, A. R., Pessin, J. E., Courtney, C. H., & Olefsky, J. M. (2007). Insulin Resistance. *Mechanisms of Insulin Action: Medical Intelligence Unit*, 185-209.

Schütten, M. T., Kusters, Y. H., Houben, A. J., Niessen, H. E., op't Roodt, J., Scheijen, J. L., ... & Stehouwer, C. D. (2020). Glucocorticoids affect metabolic but not muscle microvascular insulin sensitivity following high versus low salt intake. *JCI insight*, *5*(6): e127530.

Shakeri, H., Azimian, A., Ghasemzadeh-Moghaddam, H., Safdari, M., Haresabadi, M., Daneshmand, T., & Namdar Ahmadabad, H. (2022). Evaluation of the relationship between serum levels of zinc, vitamin B12, vitamin D, and clinical outcomes in patients with COVID-19. *J. med. Virol.*, *94*(1): 141-146.

Tokushige, K., Ikejima, K., Ono, M., Eguchi, Y., Kamada, Y., Itoh, Y., ... & Koike, K. (2021). Evidence-based clinical practice guidelines for nonalcoholic fatty liver disease/nonalcoholic steatohepatitis 2020. *J. Gastroenterol*, *56*(11): 951-963.

Utete, B., Mabika, N., Chiwara, J., Makaure, J., Phiri, C., Mlambo, S. S., ... & Tsamba, J. (2019). Histological alterations of selected tissues (gill, liver, kidney and stomach) in two common fish species within two eutrophic peri-urban lakes in Zimbabwe. *Afr. J. Aquat. Sci*., *44*(2): 155-162.

White, P. A., Cercato, L. M., Araújo, J., Souza, L. A., Soares, A. F., Barbosa, A. P. O., ... & Brito, L. C. (2013). Modelo de obesidade induzida por dieta hiperlipídica e associada à resistência à ação da insulina e intolerância à glicose. *Arq .Bras. Endocrinol. Metabol 57*: 339-345.

Yang, J., Li, L., An, Z., Lv, Y., Li, R., Li, J., ... & Guo, H. (2025). Role of hepatocyte-specific FOXO1 in hepatic glucolipid metabolic disorders induced by perfluorooctane sulfonate. *Envl. Pollut*., *367*:125632.

Zhang, X., Shao, H., & Zheng, X. (2019). Amino acids at the intersection of nutrition and insulin sensitivity. *Drug Discov .Today*, *24*(4): 1038-1043.

دور الميو- إينوزيتول الميو إينوزيتول في تحسين مقاومة الأنسولين المستحث في نموذج الفأر بنظام غذائي عالي الدهون

حنين محمود الجزيري ، أ.م. د. مني محمد علوان ، أ.د.هالة عبدالعظيم مصطفي، أ.د.زينب ابراهيم عطية ، أ.د.غادة عبدالحميد طبل.

قسم علم الحيوان، كلية العلوم، جامعة طنطا، مصر

تحدث مقاومة الأنسولين عندما تصبح خلايا الجسم أقل استجابة للأنسولين، وهو الهرمون الذي ينظم مستويات السكر في الدم. هذه المقاومة هي عامل رئيسي في حالات مثل داء السكري من النوع ٢ ومتلازمة المبيض المتعدد الكيسات. يُعدّ الميو إنوزيتول الميو إنوزيتول أحد أفراد عائلة فيتامين ب، وهو أحد سلائف فوسفات الإينوزيتول الذي يلعب دوراً في الإشارات الخلوية واستقلاب الجلوكوز وحساسية الأنسولين.

هذه الدراسة صُممت للتحقيق في التأثير العلاجي للمايو-إنوزيتول (myo-inositol) على مقاومة الأنسولين الناتجة عن النظام الغذائي الغني بالدهون (HFD) في فئرانC57BL/6 ؛ حيث تم قياس الوزن (B.Wt) ومحيط الخصر كل أسبوع. بالإضافة إلى ذلك، تم قياس مستوى سكر الدم الصائم(FBG) ، ومستوى الأنسولين الصائم (FI)، ومؤشرHOMA-IR ، ومستويات إنزيمات الكبد ALT وAST، ووظائف الكلى.

ولتحقيق هذا الهدف أجرينا الدراسة على ٤٩ من ذكور الفئران C57BL/6 ، مقسمة إلى :

المجموعة ١ تحتوي على ٧ فئران (مجموعة ضابطة): والتي تم تغذيتها بنظام غذائي عادي لمدة ١٤ اسبوع.

المجموعة ٢ تحتوي على٧فئران (مجموعة ضابطة تناولت الميو-اينوزيتول): والتي تم تغذيتها بنظام غذائي عادي مع الميو-اينو-زيتول عن طريق الفم بجرعة (١,٢ ملجم/جم) من الأسبوع السابع حتى نهاية التجربة. **المجموعة ٣** تحتوي على ٧فئران (مجموعة ضابطة تناولت الميتفورمن): والتي تم تغذيتها بنظام غذائي عادي مع الميتفورمن عن طريق الفم بجرعة (٢٥٠ ملجم/كجم) من الأسبوع السابع حتى نهاية التجربة. مجموعة مقاومة الأنسولين (ن=٢٨ فأر) التي تم تغذيتها بنظام غذائي عالي الدهون لمدة ٧ أسابيع. بعد تحديد الفئران المقاومة للأنسولين تم

تقسيم الفئران إلى ٤ مجموعات فرعية. **المجموعة ٤:** تحتوي على ٧ فئران (مقاومة الانسولين) مجموعة مقاومة الأنسولين دون علاج. **المجموعة ٥**: تحتوي على ٧فئران (مقاومة الانسولين + الميو-اينوزيتول) عولجت فئران مقاومة الانسولين بالميو-اينوزيتول لمدة ٧ اسابيع. **المجموعة ٦:** تحتوي على ٧فئران (مقاومة الانسولين + الميتفورمن) عولجت فئران مقاومة الانسولين بالميتفورمن لمدة ٧ اسابيع.٠ **المجموعة ٧**: تحتوي على ٧فئران (مقاومة الانسولين +الميو-اينوزيتول + الميتفورمن) عولجت فئران مقاومة الانسولين بميو-اينوزيتول مع الميتفورمن لمدة ٧ اسابيع.

بعد انتهاء فترة العلاج، تم وزن الفئران والتضحية بها، ثم تم جمع عينات الدم لتقييم مستوى الجلوكوز في الدم بعد الصيام، والأنسولين بعد الصيام، ومؤشرHOMA-IR ، وإنزيم الألانين أمينوترانسفيراز(ALT) ، وإنزيم الأسبارتات أمينوترانسفيراز(AST) ، ووظائف الكلى (الكرياتينين واليوريا). تم تسليم الكبد والكلى إلى ٧٠% إيثانول حتى المعالجة. ثم تم تجفيف الأعضاء وتثبيتها في شمع البارافين. بعد ذلك، تم قطعها إلى عينات بسمك ٥ ميكرومتر تلتها صبغة الهيماتوكسيلين والإيوزين

أظهرت النتائج أن تغذية ذكور الفئران من نوع C57BL/6 على نظام غذائي عالي الدهون (HFD) لمدة ١٤ أسبوعًا أدت إلى زيادة في الوزن (B.Wt) ومحيط الخصر، بالإضافة إلى ارتفاع في مستوى الجلوكوز في الدم الصائم (FBG) والأنسولين (FI) ومؤشر مقاومة الأنسولين .(HOMA-IR) كما أظهرت النتائج ارتفاعًا ملحوظًا في اختبارات وظائف الكبدALT) ، (AST ووظائف الكلى (الكرياتينين واليوريا).بعد علاج الفئران المصابة بمرض مقاومة الانسولين (IR) باستخدام (MI) و الميتفورمين(Met) ، و MI+Met أظهر انخفاضًا ملحوظًا في الوزن (B.Wt) ، محيط الخصر، ومعايير توازن الجلوكوز في مجموعة MI مقارنةً بمجموعتي Met و MI+Met. كما تم تقليل مستويات إنزيمات الكبد ALT و AST ووظائف الكلى بشكل ملحوظ في مجموعة MI+Metمقارنةً بمجموعتي MI وMet. أظهرت الفحوصات النسيجية تحسن في انسجة الكبد والكلي بعد معالجة الفئران المصابة بمقاومة الانسولين بالميو-اينوزيتول.في الختام، أثبتت هذه الدراسة أن الميو-إنوزيتول (myo-inositol) يمكن استخدامه كعلاج آمن وفعال لمقاومة الأنسولين.